BEAM BASED GAIN CALIBRATION FOR BEAM POSITION MONITOR AT J-PARC MAIN RING

H. Kuboki, T. Toyama, J. Takano, and M. Tejima, KEK/J-PARC, Tsukuba, Ibaraki, Japan

S. Hatakeyama, Mitsubishi Electric System & Service Co., Ltd., Tsukuba, Ibaraki, Japan

Abstract

A new beam-based method to calibrate the gains of Beam Position Monitor (BPM) at J-PARC Main Ring has been developed using Total Least Square fitting (TLS). The usefulness of TLS method is evaluated by the simulation. The gains are analyzed from the data obtained with the beam mapping for low and high beam intensities, and are determined with the accuracy within ±0.8% for right electrode and ±0.6% for up and down electrode.

BEAM POSITION MONITOR AT J-PARC MAIN RING

Beam Position Monitor (BPM) is one of the essential elements in a synchrotron facility. Beam positions measured with the BPMs are used to correct the closed orbit distortion (COD).

We define the "gain" such as the proportionality coefficient between the signal detected at the ADC and the ideal signal with no error as shown in Eqs. (1) and (2). The signal strength from a BPM electrode varies depending on 1) transmission characteristics of a long cable, 2) processing circuit, and 3) contact resistance at the connected parts. These are the origin of the gain fluctuation to be corrected by Beam Based Gain Calibration (BBGC) [1]. A conventional BBGC method was applied to the BPMs installed at J-PARC Main Ring (MR), however, the gains have not been corrected adequately because of the difference of the electrode shape. Therefore, a new BBGC method should be established.

Figure 1 shows the schematic of a BPM used at MR. The BPM has four electrodes of left (L), right (R), up (U), and down (D). The signal from each electrode is transmitted to the processing circuit BPMC and converted to the digitized signals shown as V_L, V_R, V_U, and V_D. Signal strength from each electrode of the BPM is represented as following.

$$V_L = \lambda\left(1 + \frac{x}{a}\right), \; V_R = \lambda g_R\left(1 - \frac{x}{a}\right), \quad (1)$$

$$V_U = \lambda g_U\left(1 + \frac{y}{a}\right), \; V_D = \lambda g_D\left(1 - \frac{y}{a}\right), \quad (2)$$

where g_R, g_U, and g_D are defined as relative gains of R, U, D electrodes divided by the gain of L electrode ($g_L = 1.0$), x and y denote horizontal and vertical position of the beam, respectively, λ denotes the line density of the beam charge with the unit C/mm^2, and a represents the effective radius of the inner surface of the electrode from the BPM center. Removing x/a, y/a, and λ from Eqs (1) and (2), we can obtain the relation

$$-\frac{R}{g_R} + \frac{U}{g_U} + \frac{D}{g_D} = L, \quad (3)$$

where V_L, V_R, V_U, and V_D are replaced by L, R, U, and D, respectively, for simplification. If we have n-data sets of (L_i, R_i, U_i, D_i) $(i = 1, \cdots, n)$, n relations of Eq. (3) can be expressed using matrix form as

$$\underbrace{\begin{pmatrix} -R_1 & U_1 & D_1 \\ \vdots & \vdots & \vdots \\ -R_i & U_i & D_i \\ \vdots & \vdots & \vdots \\ -R_n & U_n & D_n \end{pmatrix}}_{X} \underbrace{\begin{pmatrix} G_R \\ G_U \\ G_D \end{pmatrix}}_{G} = \underbrace{\begin{pmatrix} L_1 \\ \vdots \\ L_i \\ \vdots \\ L_n \end{pmatrix}}_{L}, \quad (4)$$

where $G = (G_R, G_U, G_D)$ are defined as the inverse of the gains $(1/g_R, 1/g_U, 1/g_D)$. Equation (4) can be represented as $X \cdot G = L$, where X and L denote $n \times 3$ matrix and n data of L_i $(i = 1, \cdots, n)$, respectively. Firstly, we calculate the solution G from Eq. (4). Then the gains (g_R, g_U, g_D) are obtained as the inverse of each element in G.

The gains are changed by a different configuration of the circuit even with the same BPM. For example, the gain changes depending on a beam intensity because the circuit configurations have to be changed to accept various signal strengths generated by different beam intensities. Here, we show the results of BBGC for two different beam intensities in **RESULTS**.
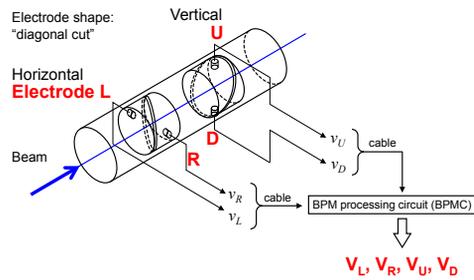

Figure 1: Diagonal-cut-type BPM at J-PARC MR.

SIMULATION

To solve Eq. (4), we have tested two methods: standard least squares fitting (LS) and total least squares fitting (TLS) [2]. We evaluated LS and TLS methods by a simulation as follows [1].

1. Gains are determined to be $(g_L, g_R, g_U, g_D) = (1.00, 1.01, 1.005, 0.975)$, which are defined as "True gain".

6: Beam Instrumentation, Controls, Feedback, and Operational Aspects

T03 - Beam Diagnostics and Instrumentation

2. The signal output voltages (L_i, R_i, U_i, D_i) $(i = 1, \cdots, n)$ are generated according to Eqs. (1) and (2) corresponding to the five horizontal beam positions as $x = -2, -1, 0, +1, +2$ mm and five vertical beam positions as $y = -2, -1, 0, +1, +2$ mm. Totally 25 (5×5) positions are prepared for data generation.

3. 500 signal data are generated at each position. Totally $n = 500 \times 25 = 12500$ data sets are prepared. The data at one position are distributed by Gaussian distribution with the relative uncertainty of $\Delta V/V = 0.2\%$ (1 sigma).

4. The data (R_i, U_i, D_i) and L_i $(i = 1, \cdots, n)$ are substituted to X and L in Eq. (4), respectively. Linear equations $X \cdot G = L$ are solved by LS and TLS methods. The gains $g = (g_R, g_U, g_D)$ are obtained from the solution G and are evaluated for LS and TLS methods.

Generally, LS method solves the normal equations as following.

$$\left(X^T \cdot X\right) G_{LS} = X^T L, \tag{5}$$

$$G_{LS} = \left(X^T \cdot X\right)^{-1} X^T L, \tag{6}$$

where X^T is the transposed matrix of X and $\left(X^T \cdot X\right)^{-1}$ denotes the inverse matrix of $\left(X^T \cdot X\right)$. The normal equation for TLS method has a form slightly changed from the Eq. (5) and (6) as

$$\left(X^T \cdot X - \sigma I\right) G_{TLS} = X^T L, \tag{7}$$

$$G_{TLS} = \left(X^T \cdot X - \sigma I\right)^{-1} X^T L, \tag{8}$$

where σ represents the eigen value of the 4×4 matrix $\left[(X \mid L)^T \cdot (X \mid L)\right]$ and I denotes unit matrix [2]. The eigen value σ has a meaning of the sum of the squared distance between each datum (L_i, R_i, U_i, D_i) and the four-dimensional plane expressed as $-RG_R + UG_U + DG_D - L = 0$. The gains obtained by LS and TLS methods (g_{LS} and g_{TLS}) are listed in Table 1 along with the true gains. In addition, the positions reconstructed using g_{LS} and g_{TLS} are plotted in Fig. 2. The positions calculated by not-corrected-gains of $(g_R, g_U, g_D) = (1.0, 1.0, 1.0)$, g_{LS}, and g_{TLS} are plotted by black, blue, and red solid circles, respectively. The g_{TLS} values successfully reproduce the true gains and the reconstructed positions are consistent with the mapping positions $(-2 \le x \le 2, -2 \le y \le 2)$. We concluded TLS method to be useful for BBGC.

Table 1: Gains Obtained by LS and TLS Methods

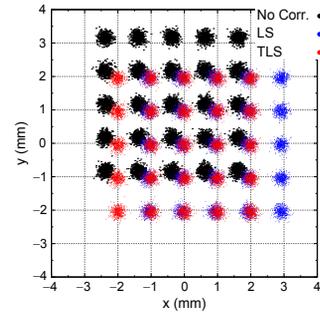|	g_R	g_U	g_D
True	1.010	1.005	0.975
g_{LS}	1.034	1.015	0.988
g_{TLS}	1.012	1.005	0.977

Figure 2: Reconstructed positions using 1) not corrected gains (black), 2) gains obtained by LS method (blue), and 3) gains obtained by TLS method (red).

ANALYSIS

We calculated the gains from the data obtained with actual beam. In order to obtain the data with mapped beam positions as in the simulation, the circulating beam orbit was kicked by a steering magnet. Figure 3 shows the applied kick angles. The kick angles are $\pm 0.4, \pm 0.2, 0$ (mrad) for one dimensional kick of horizontal (x') and vertical (y') directions, and for (x', y') case, $(\pm 0.2, \pm 0.2)$ and $(\pm 0.2, \mp 0.2)$ are applied. Totally 14-position data were obtained for each BPM. However, some BPMs locate where the beam position does not change even with a large kick angle (node of the orbit). We obtained additional data using another steering magnet located where the phase of the beam orbit differed by 90 degrees. Besides, we obtained 9 data set for each position, then, totally $n = 14$ points $\times 2$ sets $\times 9$ data = 252 data were used for fitting.

Obtained wave form data were Fast-Fourier-Transformed and the signal strength at the frequency of 3.34 MHz, which was the second harmonic of the RF frequency, was used as the signal data (L_i, R_i, U_i, D_i) $(i = 1, \cdots, n)$.
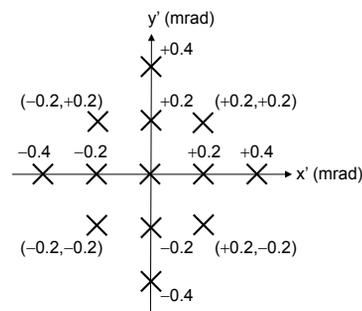

Figure 3: Beam mapping condition.

RESULTS

The gains g_R, g_U, and g_D are plotted in Fig. 4 (a), (b), and (c), respectively, as a function of the address number along MR. The gains for two cases of beam intensities (low

and high) are plotted as blue and red solid circles, respectively. The beam amounts of "Low" and "High" intensities are 10^{13} and 10^{14}-order protons per pulse, respectively. The gains are different by maximally 2–3% between the cases of "Low" and "High" intensity. The accompanied error bars are calculated as following. If we define the generalized inverse matrix $\left(X^T \cdot X - \sigma I\right)^{-1}$ as α^{-1}, the diagonal components $\left(\alpha^{-1}\right)_{11}$, $\left(\alpha^{-1}\right)_{22}$, and $\left(\alpha^{-1}\right)_{33}$ correspond to the square of the relative errors of G_R, G_U, and G_D, respectively. If we assume the uncertainties of each data (L_i, R_i, U_i, D_i) $(i = 1, \cdots, n)$ are same, the averaged uncertainty can be expressed by σ in Eq. (8). The uncertainties of $g_R = 1/G_R$ is calculated as following.

$$(\Delta g_R)^2 = \left(\frac{\partial g_R}{\partial G_R}\right)^2 (\Delta G_R)^2, \tag{9}$$

$$= \left(\frac{1}{G_R^2}\right)^2 \left(\left(\alpha^{-1}\right)_{11} \frac{\sigma}{n}\right) = \frac{\left(\alpha^{-1}\right)_{11}}{G_R^4} \frac{\sigma}{n}, \tag{10}$$

Typical uncertainties of the gains are 0.8% for g_R and 0.6% for g_U and g_D. Here, since we assume the uncertainty of $\Delta g_L = 0$, the uncertainty of g_R includes Δg_L and becomes $\sqrt{2}$ times larger than Δg_U and Δg_D.

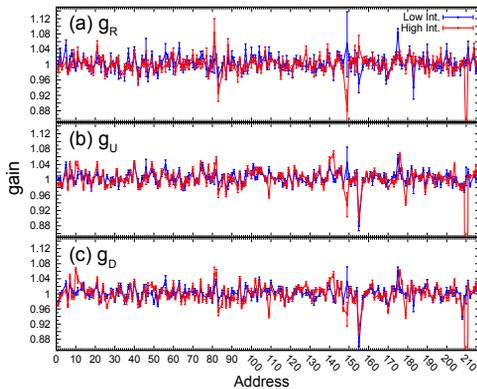To evaluate the analyzed gains, we checked the consis-

Figure 4: Gains calculated by TLS method as a function of the address number. (a) g_R, (b) g_U, and (c) g_D are plotted with their uncertainties.

tencies of four positions calculated from Eqs. (1) and (2) as following.

$$x_0 = \frac{L - R/g_R}{L + R/g_R} a, \quad y_0 = \frac{U/g_U - D/g_D}{U/g_U + D/g_D} a, \tag{11}$$

$$x_1 = \frac{L - R/g_R}{U/g_U + D/g_D} a, \quad y_1 = \frac{U/g_U - D/g_D}{L + D/g_D} a, \tag{12}$$

$$x_2 = \left(\frac{2L}{U/g_U + D/g_D} - 1\right) a, \quad y_2 = \left(\frac{2U/g_U}{L + R/g_R} - 1\right) a, \tag{13}$$

$$x_3 = \left(1 - \frac{2R/g_R}{U/g_U + D/g_D}\right) a, \quad y_3 = \left(1 - \frac{2D/g_D}{L + R/g_R}\right) a, \tag{14}$$

where (x_0, y_0) is the position used for practical operation and (x_1, y_1)–(x_3, y_3) are obtained from different form using two or three electrodes. (x_0, y_0)–(x_3, y_3) of one BPM (#015) are plotted in Fig. 5 (a) and (b) for now used gains and newly analyzed gains, respectively. (x_0, y_0), (x_1, y_1), (x_2, y_2), and (x_3, y_3) are plotted by red, green, blue, and pink solid circles, respectively. The center of the positions calculated from analyzed gains are consistent among (x_0, y_0)–(x_3, y_3), while those of used gains show discrepancies. The tilted correlation between x and y positions observed for (x_2, y_2) and (x_3, y_3) are caused by the fluctuation of λ in Eqs. (1) and (2).
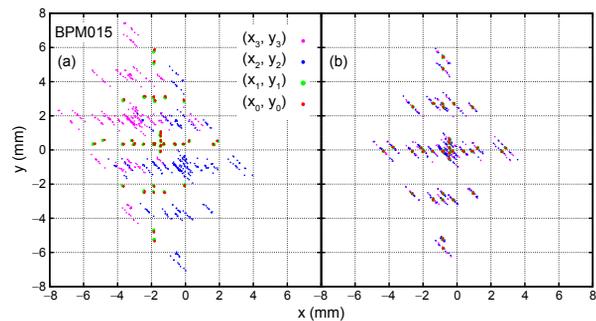

Figure 5: Consistency check.

SUMMARY

The new BBGC method for BPMs at J-PARC MR has been developed using TLS fitting. The simulation results show the usefulness of applying TLS method. The mapping data have been analyzed and the gains were obtained for "Low" and "High" intensity cases with an accuracy of 0.8% for g_R and 0.6% for g_U and g_D. Consistency is checked for four positions calculated by different form and it is found that the positions obtained by the analyzed gains successfully show the consistency. In near future, the COD correction for practical operation will be tested with the analyzed gains.

ACKNOWLEDGMENT

REFERENCES

[1] M. Tejima et al., "Beam Based Gain Calibration of Beam Position Monitors at J-PARC MR", DIPAC'11, Hamburg, Germany (2011).

[2] Ivan Markovsky and Sabine Va Huffel, "Overview of total least squares methods", Signal Processing 87, 2283-2302 (2007).